CIRP Annals - Manufacturing Technology xxx (2016) xxx–xxx

Contents lists available at ScienceDirect

CIRP Annals - Manufacturing Technology

journal homepage: http://ees.elsevier.com/cirp/default.asp

Thermo-mechanical modeling of the third deformation zone in machining for prediction of cutting forces

Erhan Budak (1)[a,*], Emre Ozlu [b], Hayri Bakioglu [a], Zahra Barzegar [a]

[a] Sabanci University, Manufacturing Research Laboratory, Istanbul, Turkey
[b] Maxima Manufacturing R&D Ltd., GOSB TechnoPark, Kocaeli, Turkey

ARTICLE INFO

Keywords:
Cutting
Modelling
Edge forces

ABSTRACT

Third deformation zone in machining arises due to contact between the cutting edge and the work material resulting in edge forces. Contribution of edge forces can be significant for cases involving large cutting edge radii or small feed rates. In this study, a thermo-mechanical modelling of the third deformation zone is presented with applications. The model eliminates the need for extensive number of calibration tests for identification of these coefficients. Effects of cutting edge geometry and process conditions on the edge forces are investigated through measurements and predictions. The application of the model to micro milling operations is also demonstrated.

1. Introduction

Cutting edge radius at the cutting edge of the tool results in the third deformation zone which may have significant contributions to the cutting mechanism [1,2]. The third deformation zone in metal cutting appears due to recovery of the ploughed material [3,4] under the stagnation angle [5] which separates the chip formation and the finished part surface. Understanding and modelling of the third deformation zone mechanics are necessary especially for high precision and micro machining operations due to very low chip thickness which increases the contribution of this zone.

For modelling of the forces due to ploughing, slip-line field theory [5,6] and finite element simulations [7] have been used. In this study, the thermo-mechanical model developed for the primary and the secondary deformation zones [8] is applied to the third deformation zone considering the high accuracy, low simulation time and limited number of calibration tests required in this approach. The flank contact is modelled considering sticking and sliding zones determined by the help of the normal pressure distribution, and verified by contact length and force measurements. A new experimental procedure is developed to identify the third deformation zone forces by a single experiment which is validated by the traditional linear regression analysis performed on number of cutting test results. The effect of the tool edge geometry and cutting parameters on the third deformation zone forces is investigated using the proposed method and the experimental data. The application of the model is demonstrated on micro milling examples where the effect of third deformation is significantly higher compared to conventional cutting operations.

2. Modelling of the primary, secondary and third deformation zones

This section summarizes the thermo-mechanical modelling approach used to predict the cutting forces in the primary, secondary and the third deformation zones.

2.1. Modelling of the primary and the secondary deformation zones

The primary deformation zone is modelled by using Johnson–Cook constitutive equation in the thermo-mechanical cutting process model presented in [8]:

$$\tau = \frac{1}{\sqrt{3}}\left[A + B\left(\frac{\gamma}{\sqrt{3}}\right)^{n}\right]\left[1 + \ln\left(\frac{\dot{\gamma}}{\dot{\gamma}_0}\right)^{m}\right][1-(\overline{T})^{v}] \quad (1)$$

where γ is the shear strain, $\dot{\gamma}$ is the shear strain rate, $\dot{\gamma}_0$ is the reference shear strain rate, A, B, n, C and m are the material constants and $\overline{T}$ is the reduced temperature. The secondary deformation zone, on the other hand, is represented by a dual-zone contact model [8] due to the existence of both sticking and sliding friction under high normal stresses on the rake face. The total contact length on the rake face can be predicted by the following equation derived from the force and moment equilibrium of the chip which is exposed to normal and frictional forces [8]:

$$l_c = f\frac{\zeta+2}{2}\frac{\sin(\emptyset+\lambda_a-a)}{\sin\emptyset\cos\lambda_a} \quad (2)$$

where f (mm) is the uncut chip thickness, ζ is the normal stress distribution exponent, and $\emptyset$, λ_a and a are the shear angle, friction angle and rake angle, respectively. It has been shown in [8] that the thermo-mechanical model can be used to predict primary and secondary zone forces accurately for various cutting conditions and rake angles without extensive calibration tests once the

* Corresponding author.
E-mail address: ebudak@sabanciuniv.edu (E. Budak).

http://dx.doi.org/10.1016/j.cirp.2016.04.110
0007-8506/© 2016 CIRP.

material constants and the dry friction between the tool and the material are known.

2.2. Modelling of the third deformation zone

The region after the stagnation point of the cutting tool is divided into three regions as illustrated in Fig. 1. The stagnation angle (θ) separates the secondary deformation zone from the third deformation. In the previous studies [5], the stagnation angle is taken in a range of 50–60°. In this study a new experimental procedure is developed for identification of stagnation angle, which is presented in Section 3.1.

The total contact length on the flank face is identified by using the full elastic recovery assumption [3,4]. In the proposed model the cutting edge radius is divided into three regions for mathematical simplification. Regions 1 and 2 are on the cutting edge radius whereas region 3 is on the flank face. Once the workpiece material moves from the stagnation point, it faces up with Region 1 which is responsible for the ploughing. Regions 2 and 3 on the other hand occur due to the elastic recovery of the material.

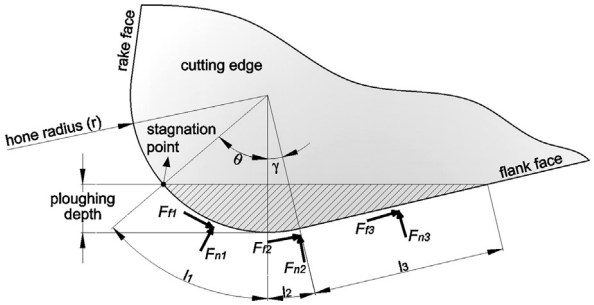

Fig. 1. Cutting edge considering the cutting edge radius in the third deformation zone.

In this approach, the total contact length on the flank face is determined as follows:

$$l_f = l_1 + l_2 + l_3 \tag{3}$$

where,

$$l_1 = \theta \cdot r \tag{4}$$

$$l_2 = \gamma \cdot r \tag{5}$$

$$l_3 = r\frac{\cos\gamma - \cos\theta}{\sin\gamma} \tag{6}$$

where θ is the stagnation angle, γ is the clearance angle, r is the cutting edge radius and l_1, l_2 and l_3 are the total contact lengths corresponding to the regions 1, 2, 3 respectively (Fig. 1).

In this study the flank contact is also modelled as a dual-zone where there exists a sticking friction contact at the regions close to the stagnation point. After a decrease on the normal pressure the contact changes to sliding. The normal pressure at the stagnation point (P_0) decreases starting from the tool tip due to free condition on the upper surface of the chip [9] and can be approximated by a cubic decay equation [8]. However, this trend may not represent the pressure conditions on the flank contact due to ploughing which pressurizes the material further. In order to investigate the normal pressure behaviour in the flank contact, various variation patterns from the tool tip were tested in the model. These can be summarized as; constant normal pressure (P_0), decreasing normal pressure as in the secondary deformation zone and increasing–decreasing pressure (Fig. 2). Based on the comparisons with the predicted and experimentally identified third zone forces, the third variation pattern was found out to describe the normal pressure variation on the flank contact most accurately. This is an expected result considering the physics of the flank contact where the material is first pressed which is followed by relaxation.

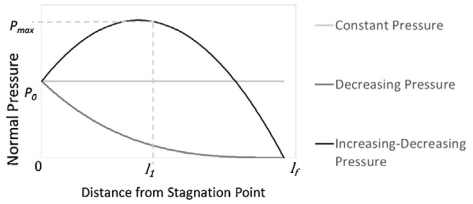

Fig. 2. Different normal pressure distributions on the flank face.

Thus, the normal pressure distribution on the flank face is represented as follows:

$$P(x) = a \cdot x^2 + b \cdot x + c \tag{7}$$

where,

$$\begin{aligned} a &= \frac{P_0}{2 \cdot l_f \cdot l_3 - l_f^2} \\ b &= -2 \cdot a \cdot l_1 \\ c &= P_0 \end{aligned} \tag{8}$$

where P_0 is the normal pressure at the stagnation point [8] and x is the distance from stagnation point.

The normal and friction forces action on the third deformation zone, can be seen in Fig. 1. The normal forces can be calculated as follows:

$$F_{Ni} = -\int_{l_i}^{l_i + l_{i+1}} w \cdot P(x) \cdot O(x) dx \tag{9}$$

where l_i is the length of the region, w is the depth of cut and $O(x)$ is the orientation function for the regions. The frictional forces must be determined depending on the contact type. If the contact condition is sticking, then the friction forces can be calculated follows:

$$F_{Fi} = \int_{l_i}^{l_i + l_{i+1}} \tau_1 \cdot w \cdot O(x) dx \tag{10}$$

where τ_1 is the shear stress at the exit of the primary deformation zone. If the contact is sliding, on the other hand, the frictional forces can be calculated as follow:

$$F_{Fi} = \int_{l_i}^{l_i + l_{i+1}} \mu \cdot P(x) \cdot O(x) dx \tag{11}$$

where μ is the experimentally identified sliding friction coefficient [8].

Total edge forces in feed and tangential directions can be calculated as follows:

$$F_{te} = \sum_{i=1}^{3} F_{Nix} + \sum_{i=1}^{3} F_{Fix} \tag{12}$$

$$F_{fe} = \sum_{i=1}^{3} F_{Niy} + \sum_{i=1}^{3} F_{Fiy} \tag{13}$$

3. Experimental verification of the proposed model

3.1. Stagnation angle prediction

In this study, a new identification method for the stagnation angle has been developed. The method is based on the milling kinematics where the uncut chip thickness varies with the immersion angle. In up-milling operations, before the critical angular position, chip is not formed and ploughing occurs (Fig. 3). After the critical angular position, the chip formation starts and all three deformation zones take place.

In order to identify the critical angular position, up-milling tests were conducted on Kern Evo CNC milling center where the cutting forces were measured by Kistler 9256C type mini dynamometer.

Please cite this article in press as: Budak E, et al. Thermo-mechanical modeling of the third deformation zone in machining for prediction of cutting forces. CIRP Annals - Manufacturing Technology (2016), http://dx.doi.org/10.1016/j.cirp.2016.04.110